RJC

RASĀYAN *J. Chem.*
Vol. 17 | No. 3 |1163-1173| July - September | 2024
ISSN: 0974-1496 | e-ISSN: 0976-0083 | CODEN: RJCABP
http://www.rasayanjournal.com
http://www.rasayanjournal.co.in

SYNTHESIS, CHARACTERIZATION, AND ANTIMICROBIAL APPLICATION OF SILVER-INCORPORATED SUPER ABSORBENT GELATIN-BASED NANOGELS

Deepak Ram[1], Rohini Dharela[1,✉], Tilak Raj[1], Sangeeta Kumari[2] and Ghanshyam S. Chauhan[3]

[1]Department of Chemistry, School of Sciences, A. P. Goyal Shimla University, Shimla, Himachal Pradesh, India-171013

[2]Department of Zoology, University of Lucknow U.P. 226007

[3]Department of Chemistry, Himachal Pradesh University, Summerhill, Shimla, Himachal Pradesh, India-171005

✉Corresponding Author: rohinidharela@gmail.com

ABSTRACT

Nanogels (Ngl) have emerged as one of the most prominent and convenient systems to act as site-specific drug delivery systems and antimicrobial agents for a varied range of diseases. Super absorbent silver incorporated gelatine-based nanogel (Ngl) grafted with acrylic acid (AAc) (gelatin-grafted-acrylic acid) (SGlAsTC) was synthesized by the chemical polymerization method for use as antimicrobial agents and prospective drug delivery matrices. The nanogel was synthesized employing *N, N*, Methylene bisacrylamide as a crosslinker and TEMED (*N, N, N,N*-Tetramethylethylenediamine) as a surfactant. The thus obtained Ngl was characterized by particle size analysis (DLS), FT-R, XRD, EDX, FESEM, and DSC to get evidence of nanogel synthesis. FTIR analysis confirmed the crosslinking reaction with AAc of Ngl, and the spherical morphology studies of SGlAsTC were confirmed by the FESEM image, which showed a sphere-like morphology with porous and crumpled particles. A swelling study was carried out at different pHs (2.2, 4.2, 6.5, 7.4, and 8.2) and at two different temperatures (at 25°C and 37°C) to evaluate the water absorption ability of the synthesized Ngl. The synthesized Ngl was subjected to antimicrobial studies against four different bacteria, exhibiting an exceptional inhibition zone for SGlAsTC against *Pseudomonas aeruginosa*. Excellent results were observed for SGlAsTC against the bacteria compared to the positive control (azithromycin). The results could be attributed to gelatin molecules that facilitated the absorption of the silver-incorporated AAc chains into the bacterial cell wall and speeded up the destruction of the cell cytoplasm.

Keywords: Antibacterial Activity, Gelatin, Nanogels, Superabsorbent.

RASĀYAN *J. Chem.*, Vol. 17, No.3, 2024

INTRODUCTION

In the contemporary landscape of nanomedicine, which encompasses the convergence of nanotechnology, medicine, and pharmaceuticals, nanogels have emerged as a viable means for transporting and dispensing medications to patients.[1-3] Considering the pressing need for significant enhancements in existing therapies and diagnostic procedures, nanotechnology plays a crucial role in developing advanced pharmaceuticals. It serves as a platform for improved drug delivery systems, cutting-edge imaging techniques, scaffolding and bone replacement, medical tools, and applications in cancer treatment, appetite control, diagnostic tests, hormone therapy, cholesterol management, immunosuppression, and tailored prescriptions for specific illnesses.[4] Within this framework, nanoparticles in the form of nanogels, multifunctional polymer-based materials, demonstrate a remarkable capacity to adjust their properties, thereby exhibiting significant potential in the realms of nanomedicine, pharmaceutics, and bio-nanotechnology. Nanogels possess the combined attributes and functionalities of both nanomaterials and hydrogels.[5] They are recognized as nano-medicinal products, having three-dimensional polymer networks characterized by a substantial water or biological fluid content. They exhibit exceptional stability, high drug loading capacity, biological consistency, strong penetration ability, and the capability to respond to environmental stimuli.[6] The integration of biopolymer-synthesized nanogels contributes to advancements and expansion in clinical investigations within the field of nanotechnology.[7] To date, a significant number

of nanogels have been created to meet growing demands across various fields. Hence, it is imperative to consolidate information on current preparation methods, physicochemical and biological properties, as well as recent applications of nanogels. Such a summary could prove valuable in exploring novel developmental pathways for nanogels.[8] Demonstrating excellent biocompatibility and resembling the native extracellular matrix, these materials blend the mechanical attributes of both solids and fluids. Consequently, they have been widely employed in regenerative medicine for many years. Among nanocarriers, naturally derived polymeric nanoparticles, particularly gelatin, stand out as efficient, cost-effective, and environmentally friendly sources.[9] The increasing interest in nanoscale materials that are biocompatible, biodegradable, and nontoxic has spurred advancements in the research field focused on the development of novel polymer nanomaterials.[10-12] The appropriate combination of nanoscale with natural polymers may lead to hydrogels.[13-19] Nanogels are unique biomaterials characterized by a three-dimensional structure created through physical or chemical crosslinking with soft hydrophilic macromolecular chains. These structures possess the capability to swell, accommodating a significant amount of water without dissolution while maintaining their integral structure.[20] While existing antimicrobial agents can help control microbial diseases, their efficacy is compromised by drug-resistant microorganisms, and they may pose environmental hazards. Gelatin and acrylic acid (AAc), on the other hand, stand out as highly versatile and commonly utilized polymeric materials.[21,22] Derived from natural sources, gelatin exhibits biocompatibility, biodegradability, and non-toxicity. Enhancing the performance of nanogels is crucial, and to achieve this, chemical modifications such as crosslinking must be used on the polymer.[23-29] The present work aims to synthesize new silver-incorporated gelatin-based AAc branched *N,N*-methylenebisacrylamide (MBAm) crosslinked nanogels for antimicrobial application and potential use as drug delivery devices.[30-34]

EXPERIMENTAL

Materials

Silver Nitrate($AgNO_3$) (MW 169.87) [Avantor Performance Materials India Limited], Gelatin, Acrylamide (AAm 99%) [Fisher Scientific India Pvt. Ltd.],*N,N*- Methylenebisacrylamide (MBAm 99%, MW 154.17) [Loba Chemie], Ammonium persulphate (APS 99%, MW 228.19) [Loba Chemie] and Sodium Lauryl Sulphate/Sodium Dodecyl Sulphate (SDS Needle shape extra pure 91%, MW 288.38) [Loba Chemie] were used as obtained. Sodium hydroxide (NaOH)(MW 40) [Themo Fisher Scientific India Pvt.Ltd.], Cyclohexane (99% MW 84.16) [Loba Chemie], and Acetone (99% MW 58.08) [Qualikems Fine Chem Pvt. Ltd.], and a Sonicator (Digital Ultrasonic Cleaner, 80W) were used as procured.

Preparation of Gel-N, N-BAAm-*Cl*-PAAc Nanogel

For the preparation of Gel-N, N-BAAm-*Cl*-PAAc nanogel, 0.500 g of gelatin was taken in a 100 ml beaker marked with [A] and 10 ml of distilled water was added to it. The mixture was heated to 30°C with continuous stirring, followed by the addition of 0.21 g of NaOH. Took 0.500 g of Acrylamide (AAm) in another 100 ml beaker [B], with 10 ml of DW and 0.047 g of Ammonium persulphate (APS), mixed it well, and then added crosslinking agent 0.152 g of MBAm. Mix the materials of beaker A and beaker B solutions, along with 0.01 g of surfactant (SDS) and 0.008 g of $AgNO_3$ solution (with 5 ml of distilled water), to obtain a homogeneous solution. The above mixture was continuously stirred on a magnetic stirrer for 15 minutes. To the homogeneous solution, 15 ml of cyclohexane was added, and the mixture was sonicated for 15 minutes at 75°C followed by sonicating the mixture for 2-3 hours at 65-75°C. The resulting SGlAsTC nanogel was thus obtained by extraction using acetone. The extracted nanogels were dried in a hot air oven at 45°C for 72 hours without disturbance. The dried nanogel thus obtained was labeled as Ag-[Gel-N, N-BAAm-*Cl*-PAAc] nanogel, as shown in Fig.-1 (a), (b), and Fig.-2, which depicts the schematic illustration of the synthetic route of Ag-[Gel-N,N-BAAm-*Cl*-PAAc] (SGlAsTC) nanogel.

Characterization of Synthesized Ngl

The synthesized Ag-[Gtn-*cl*-*N,N*-MBA-AAs] nanogel was characterized by various techniques to get evidence for successful synthesis and silver incorporation. The Fourier Transform Infra-Red (FTIR) spectra were reported in a wavenumber range of 400-4000 cm^{-1} as a KBr pellet by an FTIR spectrometer

(Nicole 6700, Thermo-Scientific, USA). X-ray diffraction (XRD) measurement was performed at a rate of 10 Ċ/min using an X-ray diffractometer (D8 Advance Eco, Bruker, Germany). The particle size diameter was recorded by Dynamic Light Scattering (DLS) in a Nano Zetasizer instrument with a (BI-SVK92), and a scattering angle of 173º at 25 ºC**.** The Field Emission Scanning Electron Microscope (FESEM) images were recorded by (JSM 7610F, JEOL, Japan) and Energy Dispersive X-ray Spectroscopy (EDX) analysis was performed by (JSM 6490 LV, JEOL, Japan).

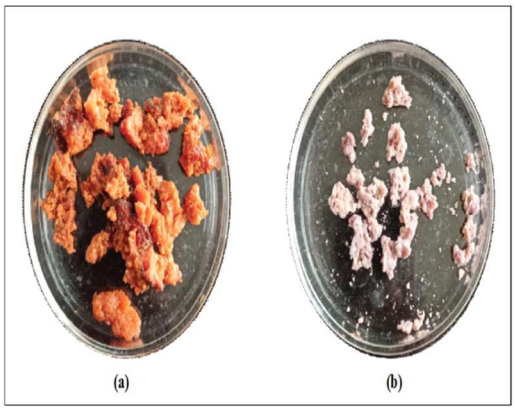

Fig.-1: (a) Dried form of Ag-[Gel-N,N-BAAm-*Cl*-PAAc] (SGlAsTC) Nanogel and (b) Swollen Form of Ag-[Gel-N,N-BAAm-*Cl*-PAAc] (SGlAsTC) nanogel

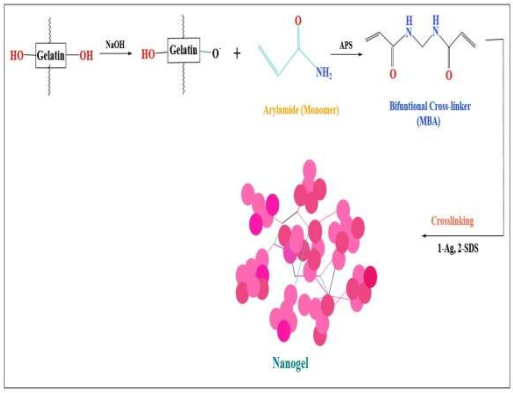

Fig.-2: The Schematic Illustration of the Synthetic Route of Ag-[Gel-N,N-BAAm-*Cl*-PAAc] (SGlAsTC) Nanogel

Swelling Study of SGIAsTC Nanogel

Materials for Swelling Study

Synthesized SGlAsTC nanogel, pH tablets of 4.0 and 7.0 pH, electronic balance BL 220H with a capacity of 220 g and readability of 0.001 g (Shimadzu Corporation Japan), water bath with thermostat, distilled water, and centrifugation machine.

Methods of Swelling Studies

To evaluate the pH sensitivity of the synthesized nanogels, swelling studies of SGlAsTC nanogel were performed around GI tract pH(at 5 different pHs such as 2.2, 4.2, 6.5, 7.4, and 8.2) and the temperature at 25 ºC and 37 ºC. The dried Ngl was used for the swelling studies. The process included weighing the weight of a 15 ml of dry empty centrifuge tube, filling it with 5 mL of a specific pH solution, reading the weight again, followed by adding 0.05 g of nanogel fine powder, and again reading the total weight of the tube. The tube was left undisturbed for 5 minutes at temperatures between 25 ºC and 37 ºC and centrifuged at 5000 rpm in a centrifugation machine for 2 minutes. Then the water content was decanted in a test tube and again centrifuged for 1-2 minutes at 5000 rpm to remove the residual water, and the weight of the swollen nanogel was calculated. Each experiment was performed in different time intervals, i.e., 5, 10, 20, 40, 80, 160, and 320 minutes, at the given temperature until an equivalent weight was obtained.

Antibacterial Activity

The antibacterial activities of the sample were evaluated using Luria Bertani agar disc diffusion, where a filtered disc was saturated with the compound and placed on the surface of inoculated agar plates. The synthesized nanogel was dissolved in DMSO to attain a 20 mg/mL solution and then filtered using a 0.22 µm Minisart syringe filter. The agar disc diffusion assay was used to determine the antimicrobial activity against four bacterial standard species, including *Pseudomonas aeruginosa* (ATCC), *Escherichia coli* (ATCC), *Staphylococcus aureus* (ATCC), and *Streptococcus mutans* (ATCC). The antimicrobial study was examined at two different doses, using Petri dishes with 90 mm on each side, sterile paper discs (6 mm in diameter) were impregnated with 20 µL of the compound solution, introduced on the inoculated upper layer of the seeded agar plates, and incubated for 16-18 hours at 37°C. The antibacterial activities of the compound were compared with the known antibiotic azithromycin (10 µg/disc) as a positive control and DMSO (20 µL/disc) as a negative control. To estimate the diameter of the zone of inhibition around the discs, it was measured by Vernier on the scale in (mm) on the surface of the plates.

RESULTS AND DISCUSSION

Spectroscopic Techniques

Fourier Transform Infrared Spectroscopy

The FT-IR spectra of Gtn and SGlAsTC were reported in a wavenumber range of 400-4000 cm^{-1} by an FT-IR spectrometer (Nicole 6700, Thermo-Scientific, USA). The FT-IR spectrum of pure Gtn in Fig.-3 (a) exhibited a broad absorption band of 3440.38 cm^{-1} due to -O─H stretching. The peak at 2929.34 cm-^{1} is assigned due to the asymmetric stretching vibration of -O─H and -C─H. The absorption spectrum showed characteristic bands of amide at 1644.98 cm^{-1} and 1536.98 cm^{-1} due to stretching of the -C═O group, together with a contribution to the distortion of the -C─N and -N─H. The bending at 1448.27 cm^{-1} and 1332.57 cm^{-1} correspond to -CH_3 and -CH_2 shows greater relative intensity. The peaks observed at 1236.14 cm^{-1} and 1078.01 cm-1 are evidence due to stretching of the -COOH group and -C─O─C stretching vibration.[1,2,35] The absorption bands near 866.36 cm^{-1} and 530.32 cm^{-1} correspond to the out-of-plane bending and stretching due to the aromatic ring.

On the other hand, the band profile of crosslinked SGlAsTC in Fig.-3 (b) was almost identical to that observed for Gtn. The FT-IR spectrum of SGlAsTC broadband 3423.02 cm^{-1} was observed due to the stretching of -O─H. The peak at 2948.62 cm^{-1} is due to the asymmetric vibration of -O─H and -C─H. The absorption band showed characteristic bands of amide at 1668.12 cm^{-1}, 1540.84 cm^{-1}, and 1396.21 cm^{-1}, due to stretching of -C═O with distortion of -C─N, -N─H, and -CH_3. In addition to the characteristic band of the biopolymer, the peaks at 1230.36 cm^{-1}, 1180.22 cm^{-1}, and 1091.51 cm^{-1} correspond to the stretching of -C─O and the presence of the crosslinker. Hence, it could be indicated that the carbonyl groups of the Gtn participate in the crosslinking reaction.

Dynamic Light Scattering

The particle size of the obtained nanogel was evaluated with a Nano Zetasizer instrument (BI-SVK92). Most of the particles are sized within the nanometric scale with Poly Dispersity Index (PDI) values between 0.27 and 0.40, and the result is shown in Fig.-3(c). The average size of the synthesized SGlAsTC up to 260 nm was observed with a degree of increasing crosslinking. The particle size relationship is attributed to the structural complexity and hydrophilicity of Gtn and the amount of crosslinker, which allows the entrance of more water into the nanogel and reaches a greater index swelling value of the material. The result is an increase in the Dh value.[36] In addition, smaller sizes were obtained from the porous structure, and the hydrophilicity of SGlAsTC, which can form a greater amount of crosslinking, could explain the smaller size of their Ngl. The crosslinking reaction of Gtn could be favored by the higher amount of amine C═O groups present in the chain relative to AAs.

X-ray Diffraction

The XRD analysis of synthesized silver incorporated SGlAsTC nanogel showed diffraction peaks at 2θ = 19.00, 23.05, 27.86, 30.94, 32.02, 33.78, 38.46, and 48.67 respectively as shown in Fig.-3(d). It was compared to the standard, and the resultant XRD spectrum confirmed that the synthesized silver incorporated nanogel is crystalline in nature and nanocrystal form. The peaks can be assigned to planes

(200), (101), (210), (110), (111), and (003) of pure silver based on the face-centered cubic structure, respectively.[37-39] According to the standard JCPDS[40] it was observed from the pattern that the copolymer has exhibited more clearly planed peaks due to the existence of Gtn molecules and hydrogen bonding by macromolecules in which chains are rearranged with more regularity, which leads to a better appearance of XRD peaks in synthesized nanogel. From the XRD result, considering the peaks at degrees, the average particle size has been determined via the Debye- Scherrer equation.

$D = 0.9\lambda / \beta\cos\theta$, ($\beta = \pi \times FWH/180$)

Where 'λ' is the wavelength (1.541 Å), 'β' FWHM (full width at half maximum), 'θ' is the diffraction angle, and 'D' is the diameter of particle size. The value of 'd' is calculated using Bragg's Law ($n\lambda = 2d\sin\theta$). The average diameter of synthesized nanogel was estimated from the Scherrer equation at 89 nm, as shown in Table-1. This result indicates that the biomaterial exists in the nanoscale structure.

Table-1: Particle Size Analysis Data Through the XRD of SGIAsTC

Peak Position (2 θ)	Theta	FWHM	Crystallite Size D (nm)	d Spacing
18.91	9.46	1.09	72.61	4.69
23.12	11.56	1.18	67.38	3.85
27.73	13.87	0.65	123.13	3.22
29.22	14.61	0.64	123.29	3.06
32.05	16.03	1.07	74.09	2.79
33.69	16.85	1.15	69.28	2.66
38.35	19.18	0.93	85.17	2.35
48.81	24.41	1.09	72.63	1.86

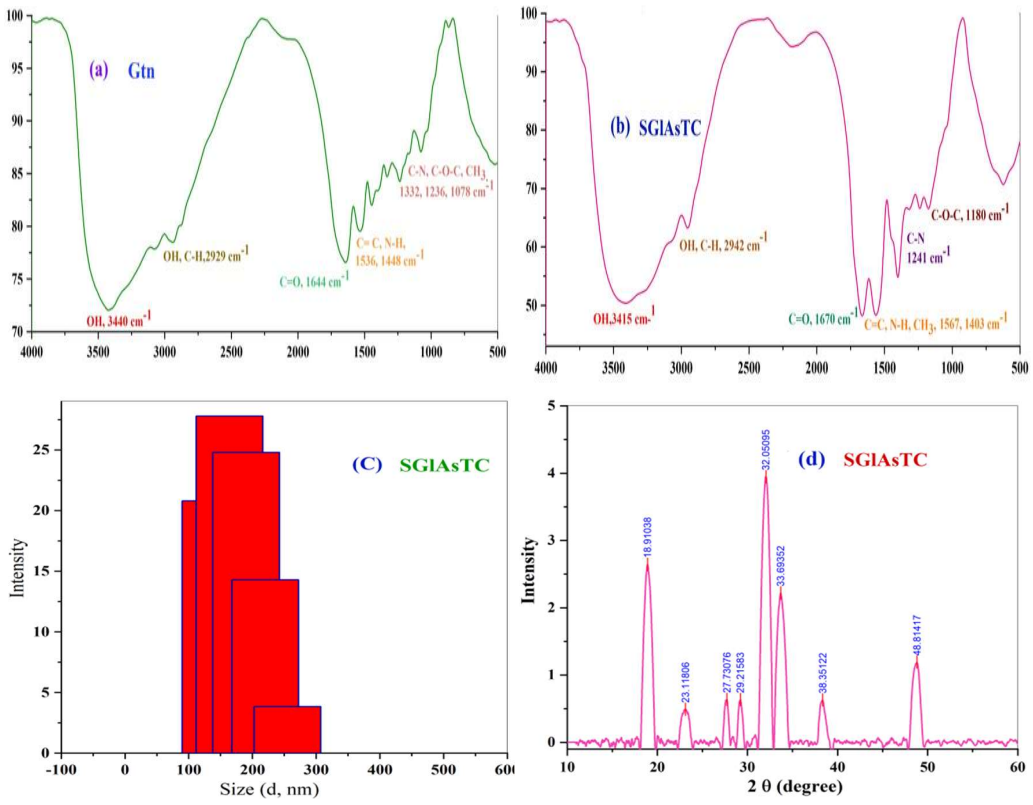

Fig.-3: (a) FTIR Spectra of Gtn, (b) FTIR Spectra of Ag-[Gel-N,N-BAAm-*Cl*-PAAc] (SGlAsTC) (c) Particle Size Analysis /DLS Of Ag-[Gel-N,N-BAAm-*Cl*-PAAc] (SGlAsTC) (D) XRD Of Ag-[Gel-N,N-BAAm-*Cl*-PAAc] (SGlAsTC)

Energy Dispersive X-ray Spectroscopy

Energy Dispersive X-ray (EDX) was used to find the elemental composition in the reaction mixture. The EDX analysis of synthesized Ngl was done by SEM (model JSM 6490 LV, JEOL, Japan). The EDX spectrum shows a signal in the silver region that confirms the formation of SGlAsTC, as shown in Fig.-4(a). The metallic silver nanocrystal generally shows a characteristic optical absorption peak around 3.0 keV due to surface plasmon resonance.[41] Silver (Ag 0.08%) was the main component as compared to other elements represented in Table-2(b). The energy dispersive spectroscopy data show a very strong signal of carbon and oxygen and a weak signal of silver due to the very small amount of silver added to the reaction mixture. The EDX peak demonstrated that the required phase of silver (Ag) is present in the sample.

Table-2: EDX Elemental Percentage in Synthesized (SGlAsTC) Ngl

Elements	Weight %	Atomic %
C K	59.26	67.91
O K	36.94	31.78
Ag L	0.60	0.08
Pt M	3.20	0.23
TOTALS	100	100

Microscopic Technique

Field Emission Scanning Electron Microscope

The surface morphology of synthesized nanogel has been proven by FESEM analysis (JEOL JSM 7610f, Japan), summarized in Fig.-4 (c) and (d). As evidenced by the SEM images, the nanogel has exhibited a spherical, oval, and porous-like morphology with crumpled particles. When comparing particle size analysis and FESEM data, the variation observed in particle size may be attributed to the fact that silver nanogel have a tendency to agglomerate due to its high surface energy and the high surface tension of the smoothy nanogel. The finer particle size results in a larger surface area, which in turn increases the catalytic activity of the nanogel.

Thermal Analysis

Differential Scanning Calorimetry

DSC is a thermal analytical instrument that measures how the physical properties of a sample change along with temperature over time. The result of the sample was obtained by using the DSC thermogram [Setaram Instrumentation, Model D649, (temp 700 Ċ to -170 Ċ), Russia] at a temperature range of 25 °C up to 300 °C and a heating rate of 10 °C/min. The first DSC heating scan of Ngl shows a baseline shift attributed to the glass transition (T_g) around 40 °C that is followed by an endotherm associated with water evaporation [42]. The thermogram shows two endothermic peaks at approximately 70.18 (°C)/308.4 (s) and 213 (°C)/1165 (s), which is associated with the melting point (T_m) of the Ngl, as shown in Fig.-4(d)[43] After quench-cooling, a second heating scan was performed and in such a scan, no endotherm due to water evaporation was evident anymore. The Ngl shows some drift at the baseline due to thermal degradation. The Tg of Ngl was expected to be higher than that in the first scan due to the fact that water acts as a plasticizer and has flexibility, but was not detectable in the second scan. This behavior is to be expected from a polymeric sample and the individual Tg behaviors of its components. Nanogel polymers could exhibit different thermal characteristics depending on the chain of Gtn, which can influence the molecular weight and consequently the physicochemical properties of the compound (such as viscosity).

Swelling Studies

Swelling is a parameter that describes the hydrophilicity or amount of water absorption in a material. Swelling is a physiochemical characteristic of conducting polymers that is responsible for water absorption and can be attributed to gelling properties, electrostatic interaction, and grafting interaction in materials. Furthermore, the swelling properties of the nanogels can be useful as drugs for anticancer activity. The swelling percentage can be determined by the swelling degree.[44]

Swelling Degree

To find out this parameter, 0.05 g of the samples have been immersed in 5 ml of water at different time intervals, and their weight has been measured after the removal of additional water.

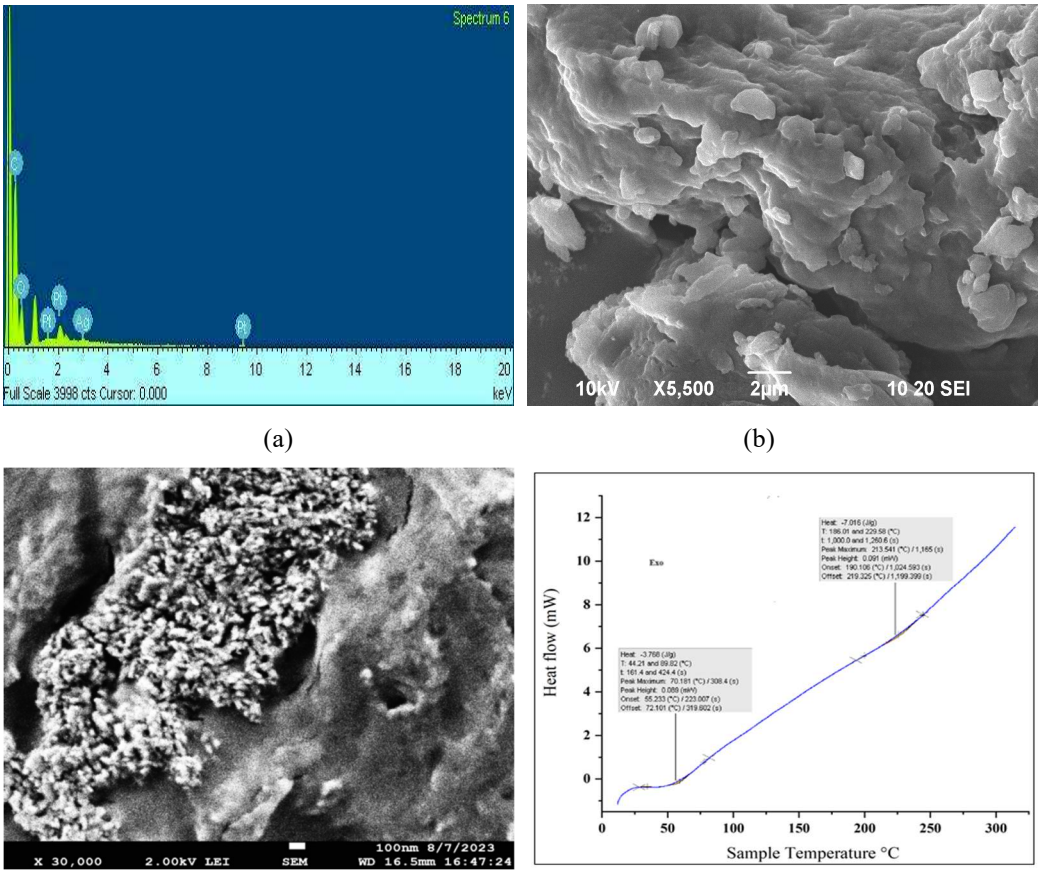

Fig.-4: (a) EDX Elemental Spectrum of Ag-[Gel-N,N-BAAm-*Cl*-PAAc] (SGlAsTC) Ngl, (b) and (c) FESEM of Ag-[Gel-N,N-BAAm-*Cl*-PAAc] (SGlAsTC) Ngl and (d) DSC of synthesized Ag-[Gel-N,N-BAAm-*Cl*-PAAc] (SGlAsTC) Ngl.

The percent of swelling (%S) is calculated from the formula given below:

$$\text{Percentage S} = [(Ws-Wd)/Wd] \times 100$$

Where 'Ws' is the swollen weight of the sample and 'Wd' is the dried weight of the sample, respectively. The swelling parameter has been demonstrated around the pH of the GI tract and at two different temperatures, i.e., 25 °C and 37 °C, as shown in Fig.-5 (a) and (b). The higher percentages of swelling are observed at pH 6.5 (at temperature 25 °C, time 320 min) and at pH 4.2 (at temperature 37 °C, time 160 min). The significant effects are noticed at pHs and temperatures, this proves that the synthesized nanogel acts as a super absorbent. In some cases, the percent swelling increases and then decreases due to rupturing of the polymeric chain, as shown in Tables-(3) and (4). Because of the influence of temperature and pH, which causes pHs and temperatures, the bonds of hydrogen break and form simultaneously with the polymeric chain, which creates a cavity for holding the solvent molecules and releases the excess water back. From these results, we observed that the nanogel retains only those molecules that help maintain equilibrium under different forces, which depend on porosity and particle size. Due to more polar sites and more electrostatic interaction between water molecules and copolymers, this confirms that synthesized nanogel is a super absorbent.

Antibacterial Activity

The antibacterial activities of the synthesized nanogel were measured via Luria Bertani agar disc diffusion with two different types of bacteria, i.e., gram-negative *(Pseudomonas aeruginosa, Escherichia coli)* and gram-positive (*Staphylococcus aureus*, *Streptococcus mutans*).

Table-3: Showing the Values of % Swelling at pHs 25 °C

Swelling study of SGlAsTC at temp 25 Ċ					
Duration ↓	% Swelling values at different pHs				
	pH 2.2	pH 4.2	pH 6.5	pH 7.4	pH 8.2
5 Minutes	1263	1234	3072	1792	1874
10 Minutes	1385	1416	3158	1824	1968
20 Minutes	1412	1640	3242	1858	2034
40 Minutes	1432	1677	3256	1846	2076
80 Minutes	1451	1685	3286	1830	2096
160 Minutes	1446	1679	3290	1788	2112
320 Minutes	1444	1675	3290	1786	2114

Table-4: Showing the Values of % Swelling at pHs 37 °C

Swelling study of SGlAsTC at temp 37 Ċ					
Duration ↓	% Swelling values at different pHs				
	pH 2.2	pH 4.2	pH 6.5	pH 7.4	pH 8.2
5 Minutes	1029	1623	1774	1610	1766
10 Minutes	1153	1729	1826	1684	1766
20 Minutes	1173	1783	1826	1706	1788
40 Minutes	1427	1792	1854	1754	1822
80 Minutes	1463	1898	1900	1758	1878
160 Minutes	1467	1917	1904	1764	1886
320 Minutes	1465	1915	1904	1762	1888

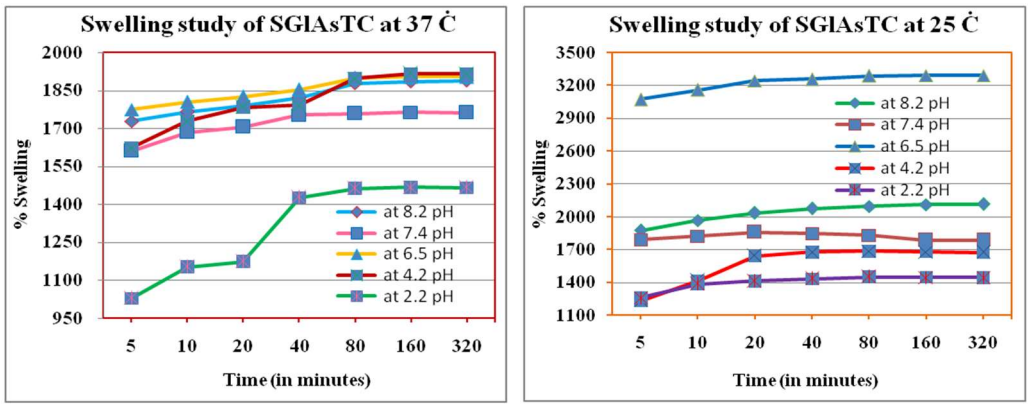

(a) (b)

Fig.-5: Curves (a) and (b) Represented the Swelling Degree of the Synthesized Ngl at various Ph.

The antibacterial activities of the synthesized Ngl were compared with a known antibiotic, azithromycin, at two different concentrations (10 and 20 µg/disc) as a positive control. The antibacterial images are displayed in Fig.-6, and the obtained results are reported in Table-5. The antibacterial analysis showed a more desirable inhibition zone, especially in *Pseudomonas aeruginosa.* No effect of the positive control (Azithromycin) was observed in this bacterial activity, whereas a much better result was observed for synthesized Ngl. Due to its resistance to azithromycin and its higher hydrophobicity, it represents better antibacterial activity. As can be observed, the antibacterial activity of SGlAsTC is due to its redox and dopant nature, which repel bacteria through electrostatic interaction with the cellular wall of the bacteria.[45-47] Due to its more hydrophobic nature, it has more antibacterial properties. The result can be associated with the fact that the existence of Gtn, due to having hydroxyl groups, helps to facilitate the diffusion of nanoparticles into the inside bacterial cell membranes, thereby preventing cell growth by

destroying its cytoplasm. The antimicrobial activity reveals that the synthesized Ngl is resistant to azithromycin.

Table-5: The Zone of Inhibition for Antibacterial Activity of Ngl

		GRAM-NEGATIVE		GRAM POSITIVE	
BACTERIAS →		*Pseudomonas aeruginosa*	*Escherichia coli*	*Staphylococcus aureus*	*Streptococcus mutans*
Samples	Conc.	Zone of inhibition		Zone of inhibition	
SGlAsTC	10 µg	5 mm	0 mm	0 mm	0 mm
	20 µg	10 mm	5 mm	6 mm	6 mm
Azithromycin	10 µg	0 mm	19 mm	23 mm	21 mm

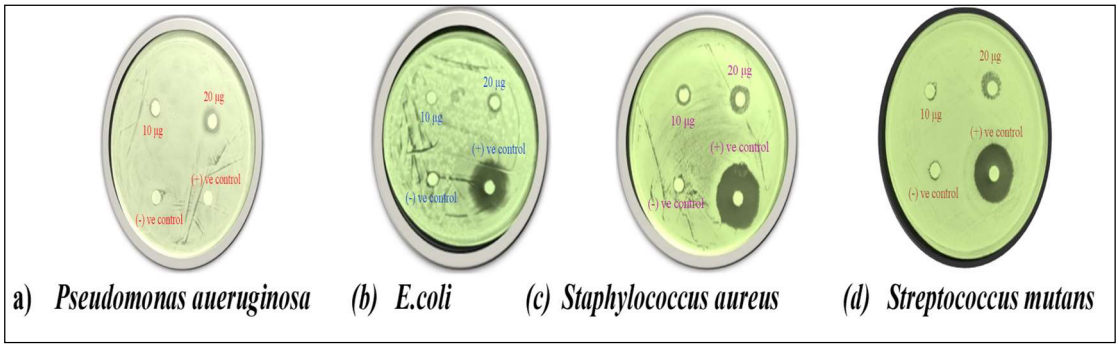

Fig.-6: The Images are Related to the Antibacterial Activity of NgI

CONCLUSION

The present work reports the successful synthesis of copolymerized nanogel via the chemical polymerization method. The nanogel was further characterized by various techniques, with DLS and FESEM supporting the nanostructure formation. The synthesized nanogel showed desirable thermal properties for DSC as a conductive composite. The physiochemical properties, such as the swelling study conducted, helped to evaluate the hydrophilicity. Due to the more polar sites and more electrostatic interaction between water molecules and copolymers, the synthesized nanogel acted as a super absorbent. The antibacterial activity of the Ngl with two different concentrations on gram-negative (*Pseudomonas aeruginosa*, *Escherichia coli*) and gram-positive (*Staphylococcus aureus*, *Streptococcus mutans*) was measured using the Luria Bertani agar disc diffusion method. The Ngl showed excellent antimicrobial activity against *Pseudomonas aeruginosa,* with a desirable inhibition zone being observed as against the positive control (azithromycin). The presence of gelatin incorporated into one moiety ensured better infusion into the cellular walls of bacteria, enhancing bacterial destruction and preventing any further growth**.**

ACKNOWLEDGEMENTS

No financial assistance/grant has been taken to carry out this work. This research work has been done on a self-finance basis.

CONFLICT OF INTERESTS

The authors declare that there is no conflict of interest.

AUTHOR CONTRIBUTIONS

All the authors contributed significantly to this manuscript, participated in reviewing/editing and approved the final draft for publication. The research profile of the authors can be verified from their ORCID ids, given below:

Deepak Ram http://orchid.org/0009-0007-3534-5681
Rohini Dharela http://orchid.org/0000-0002-8526-7585
Tilak Raj http://orchid.org/0009-0007-3534-5681
Sangeeta Kumari http://orchid.org/0000-0002-3210-4475
Ghanshyam S. Chauhan http://orchid.org/0000-0002-5032-5706

REFERENCES

1. T. Raj, R. Dharela and G.S. Chauhan, *American Journal of Innovation in Science and Engineering*, **2(1)**, 57(2023), https://doi.org/10.54536/ajise.v2i1.1288
2. T. Raj, R. Dharela, P. Chauhan and G.S. Chauhan, *Material Today., Proceedings*, **9**, 224(2022), https://doi.org/10.1016/j.matpr.2022.09.224
3. M.L. Etheridge, S.A. Campbell and A.G. Erdman, *Nanomedicine: Nanotechnology, Biology and Medicine*, **9(1)**, 1(2013), https://doi.org/10.1016/j.nano.2012.05.013
4. S.K. Sahoo and V. Labhasetwar, *Drug Discovery Today*, **8(24)**, 1112(2003), https://doi.org/10.1016/s1359-6446(03)02903-9
5. N. Wen, S. Lü, X. Xu, P. Ning, Z. Wang, Z. Zhang, C. Gao, Y. Liu and M. Liu, *Materials science & engineering. C, Materials for Biological Applications*, **100**, 94(2019), https://doi.org/10.1016/j.msec.2019.02.08
6. R. Dharela, A. Kaushik and G.S. Chauhan, *Rasayan Journal of Chemistry*, Special Issue, 273(2022), http://doi.org/10.31788/RJC.2022.1558166
7. R. Rakhshaei, H. Namazi, H. Hamishehkar, H.S. Kafil and R. Salehi, *Journal of Applied Polymer Science*, **136**, 1(2019), https://doi.org/10.1002/app.47590
8. R. Shanmuganathan, T.N.J.I. Edison, F. Lewis Oscar, P. Kumar, S. Shanmugam and A. Pugazhendhi, *International Journal of Biological Macromolecules*, **130**, 727(2019), https://doi.org/10.1016/j.ijbiomac.2019.02.060
9. M. Winnacker, *Biomaterials Science,* **5(7)**, 1230(2017), https://doi.org/ 10.1039/c7bm00160f
10. P.R. Sarika and N.R. James, *International Journal of Biological Macromolecules*, **76**, 181(2015), https://doi.org/10.1016/j.ijbiomac.2015.02.038
11. A.E. Ekkelenkamp, M. R. Elzes, J. F. J. Engbersen and J. M. J. Paulusse, *Journal of Materials Chemistry B*, **6(2)**, 210(2018), https://doi.org/10.1039/c7tb02239e
12. D.M. Eckmann, R.J. Composto, A. Tsourkas and V.R. Muzykantov, *Journal of Materials Chemistry B,* **246**, 8085(2014), https://doi.org/10.1039/C4TB01141D
13. D. Dheer, D. Arora, S. Jaglan, R.K. Rawal and R. Shankar, *Journal of Drug Targeting,* **25**, 1(2017), https://doi.org/10.3109/1061186X.2016.1172589
14. K.S. Soni, S.S. Desale and T.K. Bronich, *Journal of Controlled Release: Official Journal of the Controlled Release Society*, **240**, 109(2016), https://doi.org/10.1016/j.jconrel.2015.11.009
15. H. Zhang, Y. Zhai, J. Wang and G. Zhai, *Materials Science & Engineering C,* **60** 560(2016), https://doi.org/10.1016/j.msec.2015.11.04
16. R.T. Chacko, J. Ventura, J. Zhuang and S. Thayumanavan, *Advanced Drug Delivery Reviews*, **64(9)**, 836(2012), https://doi.org/10.1016/j.addr.2012.02.002
17. F. Alhaique, P. Matricardi, C. Di Meo, T. Coviello and E. Montanari, *Journal of Drug Delivery Science and Technology*, **30**, 300(2015), https://doi.org/10.1016/j.jddst.2015.06.005
18. H. Wang, J. Qian, and F. Ding, *Journal of Materials Chemistry B*, **5(34)**, 6986(2017), https://doi.org/10.1039/c7tb01624g
19. A. Abaee, M. Mohammadian and S.M. Jafari, *Trends in Food Science and Technology,* **70,** 69(2017), https://doi.org/10.1016/j.tifs.2017.10.011
20. E. Calo and V.V. Khutoryanskiy, *European Polymer Journal*, **65**, 252(2015), https://doi.org/10.1016/j.eurpolymj.2014.11.024
21. E.H. Kim, G.D. Han, S.H. Noh, J.W. Kim, J.G. Lee, Y. Ito and T. Il Son, *Journal of Industrial and Engineering Chemistry,* **54**, 1(2017), https://doi.org/10.1016/j.jiec.2017.05.029
22. H. Mittal, S.S. Ray, B.S. Kaith, J.K. Bhatia, J. Sharma and S.M. Alhassan, *European Polymer Journal*, **109**, 402(2018), https://doi.org/10.1016/j. eurpolymj.2018.10.013

23. L. Cui, J. Jia, Y. Guo, Y. Liu and P. Zhu, *Carbohydrate Polymers*, **99**, 31(2014), https://doi.org/10.1016/j.carbpol.2013.08.048
24. F. Laffleur and B. Strasdat, *European Polymer Journal*, **118**, 542(2019), https://doi.org/10.1016/j.eurpolymj.2019.06.013
25. R.A. Muzzarelli, J. Boudrant, D. Meyer, N. Manno, M. DeMarchis and M.G. Paoletti, *Carbohydrate Polymers*, **87(2)**, 995(2012), https://doi.org/10.1016/j.carbpol.2011.09.063
26. R. A. A. Muzzarelli, *Topics in Geobiology,* 1-34(2010), https://doi.org/10.1007/978-90-481-9684-5_1
27. A. Sionkowska, B. Kaczmarek and K. Lewandowska, *Journal of Molecular Liquids*, **199**, 318(2014), https://doi.org/10.1016/j.molliq.2014.09.028
28. M. Sarem, F. Moztarzadeh and M. Mozafari, *Carbohydrate Polymers*, **93(2)**, 635(2013), https://doi.org/10.1016/j.carbpol.2012.11.099
29. A. Oryan, A. Kamali, A. Moshiri, H. Baharvand and H. Daemi, *International Journal of Biological Macromolecules*, **107(PtA)**, 678(2018), https://doi.org/10.1016/j.ijbiomac.2017.08.184
30. Y. Sasaki and K. Akiyoshi, *Chemical Record,* **10(6)**, 366(2010), https://doi.org/10.1002/tcr.201000008
31. J. Chen, N. Wang, Y. Liu, J. Zhu, J. Feng and W. Yan, *Synthetic Metals*, **245**, 32(2018), https://10.1016/j.synthmet.2018.08.006
32. R.B. Gapusan and M.D.L. Balela, *Materials Chemistry and Physics,* **243**, 122682(2020), https://doi.org /10.1016/j.matchemphys.2020.122682
33. V. Hasantabar, H. Tashakkorian and M. Golpour, *Carbohydrate Polymers*, **224**, 115163(2019), https://doi.org/10.1016/j.carbpol.2019.115163
34. N. Sahiner, S. Sagbas, N. Aktas and C. Silan, *Colloids and surfaces. B, Biointerfaces*, **142**, 334(2016), https://doi.org/10.1016/j.colsurfb.2016.03.006
35. G.N. Rimondino, E. Miceli, M. Molina, S. Wedepohl, S. Thierbach, E. Rühl and M. Calderón, *Journal of Materials Chemistry B*, **5(4)**, 866(2017), https://doi:10.1039/c6tb02001a
36. S.K. Pillalamarri, F.D. Blum, A.T. Tokuhiro and M.F. Bertino, *Chemistry of Materials,* **17(24)**, 5941(2005), https://doi.org/10.1021/cm050827y
37. S. Qiu, C. Chen, M. Cui, W. Li, H. Zhao and L. Wang, *Applied Surface Science,* **407**, 213(2017), https://doi.org/10.1016/j.apsusc.2017.02.142
38. H.K. Chaudhari and D.S. Kelkar, *Journal of Applied Polymer Science,* **62(1)**, 15(1996), https://doi.org/10.1021/ma0119326
39. M. T. B. Clabbers, M. W. Martynowycz, J. Hattne and T. Gonen, *Journal of structural biology*, X, **6**, 100078 (2022), https://doi.org/10.1016/j.yjsbx.2022.100078
40. S. Kaviya, J. Santhanalakshmi, B. Viswanathan, J. Muthumary and K. Srinivasan, *Spectrochimica Acta. Part A, Molecular and Biomolecular Spectroscopy*, **79(3)**, 594(2011), https://doi.org/10.1016/j.saa.2011.03.040
41. P.B. Sutar, R.K. Mishra, K. Pal and A.K. Banthia, *Journal of Materials Science. Materials in Medicine*, **19(6)**, 2247(2008), https://doi.org/10.1007/s10856-007-3162-y
42. E. Chiellini, P. Cinelli, E. Grillo Fernandes, el-R.S. Kenawy and A. Lazzeri, *Biomacromolecules*, **2(3)**, 806(2001), https://doi.org/10.1021/bm015519h
43. A. Olad, F. Doustdar and H. Gharekhani, *Carbohydrate polymers*, **200,** 516(2018), https://doi.org/10.1016/j.carbpol.2018.08.014
44. M. Dathe, T. Wieprecht, H. Nikolenko, L. Handel, W.L. Maloy and D.L. MacDonald, et al., *FEBS Letters,* **403(2)**, 208(1997), https://doi.org/10.1016/s0014-5793(97)00055-0
45. C. Wu, J. Wang, S. Song, Z. Wang and S. Zhao, *Progress in Organic Coatings,* **148**, 105888(2020), https://doi:10.1016/j.porgcoat.2020.105888
46. K.D. Saint Jean, K.D. Henderson, C.L. Chrom, L.E. Abiuso, L.M. Renn and G.A. Caputo, *Probiotics and Antimicrobial Proteins,* **10(3)**, 408(2018), https://doi.org/10.1007/s12602-017-9345-z
47. M. Ghasemi, T. Turnbull, S. Sebastian and I. Kempson, *International Journal of Molecular Sciences,* **22(23)**, 12827(2021), https://doi.org/10.3390/ijms222312827

[RJC-8828/2024]